RSC Advances

PAPER

Cite this: *RSC Adv.*, 2020, **10**, 32522

Thermodynamically stable vesicle formation of biodegradable double mPEG-tailed amphiphiles with sulfonate head group†

Rita Ghosh,‡[a] Joykrishna Dey *[a] and B. V. N. Phani Kumar [b]

The development of efficient, biodegradable and biocompatible surfactants has become a pressing need because of adverse effects of surface-active compounds on the aquatic environment and human health. Cleavable surfactants containing a labile functional group have the ability to eliminate some of these problems. Consequently, PEGylated amphiphiles have found widespread applications in pharmaceutics, household purposes, and drug delivery. Herein we report synthesis and characterization of two novel amphiphiles which to our knowledge are the first examples of double PEG-tailed amphiphiles with an anionic head group. Considering their chemical structure, they are expected to be biodegradable, biocompatible, milder and less irritant than conventional surfactants. The solution behavior of these newly developed amphiphiles was thoroughly investigated in aqueous buffer (pH 7.0) at 25 °C. The surface activity of the compounds in aqueous buffer was studied by surface tension measurements. The self-assembly properties were investigated by various techniques such as fluorescence and NMR spectroscopy, dynamic light scattering, transmission electron microscopy, atomic force microscopy, and isothermal titration calorimetry. Both molecules were found to be surface active in water and exhibit spontaneous vesicle formation in the absence of any additives at room temperature. As in the cases of conventional surfactants, the self-assembly is driven by the hydrophobic effect. The vesicles produced in aqueous media were shown to encapsulate hydrophobic dyes and exhibit structural transitions upon addition of salts. The sensitivity of the vesicles to change in environments qualifies them for potential use in drug delivery.

Received 27th June 2020
Accepted 3rd August 2020

DOI: 10.1039/d0ra05613h

rsc.li/rsc-advances

1. Introduction

Surfactants are very well-known for their applications in industrial, household, and pharmaceutical formulations.[1,2] Synthetic surfactant molecules usually consist of a water-soluble polar head (ionic or uncharged) and a hydrophobic tail and thus have amphiphilic character. The hydrophobic tail is usually a long, fully saturated or partially unsaturated hydrocarbon (HC) chain, but it can also have a fluorocarbon or aromatic-based composition. For example, phospholipids are biosurfactants that have two partially unsaturated hydrocarbon tails.[3] Besides surface activity amphiphilic molecules are also known to exhibit self-assembly in suitable solvents to form a wide variety of microstructures, including spherical, rod-like and disc-like micelles, reverse micelles, closed bilayer vesicles, flat bilayers, *etc.* above a critical aggregation concentration (*cac*) under different conditions.[1,4–6] The self-assembly behavior in aqueous solutions, however, depends on the chemical structure of the amphiphile as well as on the mixing ratios (for multi-component systems), temperatures, presence of additives, and so on. However, biological and industrial applications of surfactant microstructures depend on the creation of aggregates of specified size and shape. Hence, design, control, and tuning microstructure of amphiphilic molecules have become an area of active research.

It is well-known that double HC chain synthetic surfactants and phospholipids form bilayer structures in water above a very low *cac* value.[5–10] There are also reports on bilayer membrane formation by nonionic double-tailed surfactants which contain polyglyceryl as head group.[11] The growing interest on vesicular structures is largely because they have unique structure which can solubilize both hydrophilic and hydrophobic molecules within the aqueous core and bilayer membrane, respectively.

[a]*Department of Chemistry, Indian Institute of Technology Kharagpur, Kharagpur-721302, India. E-mail: joydey@chem.iitkgp.ac.in; Fax: +91-3222-255303; Tel: +91-3222-283308*

[b]*NMR, CATERS, CSIR-Central Leather Research Institute, Adyar, Chennai-600020, India*

† Electronic supplementary information (ESI) available: Supplementary data (details of synthetic procedure, ^{1}H-NMR, and ^{13}C-NMR spectra and chemical identification of the synthesized amphiphiles, representative fluorescence emission spectra of Py, ITC thermograms, plots NMR relaxation times and pulse field gradient NMR signal attenuation, and variable temperature NMR results). See DOI: 10.1039/d0ra05613h

‡ Current address: Department of Chemistry, St. Joseph's College Autonomous, Bangalore-560027, India.

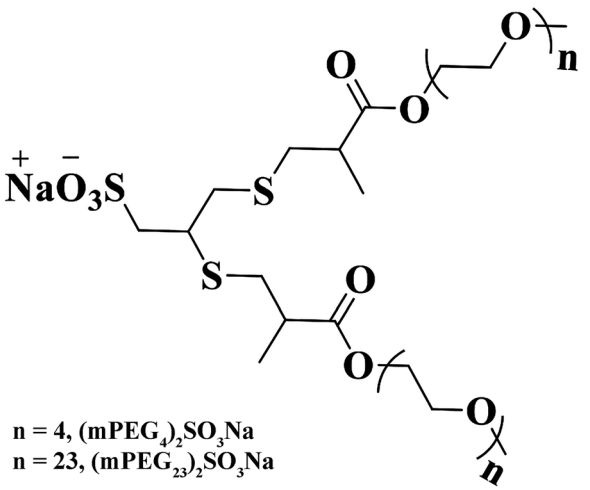

Fig. 1 Chemical structure of $(mPEG_4)_2SO_3Na$ and $(mPEG_{23})_2SO_3Na$.

Therefore, vesicles find use in pharmaceutical applications, involving drug solubilization, encapsulation, and delivery. However, for applications in biology and medicinal fields, the amphiphilic molecule must be biodegradable, non-cytotoxic, and non-immunogenic. The biodegradability and biocompatibility of amphiphiles have therefore become almost as important as their functional performance. Consequently, there is a pressing need for developing efficient amphiphiles that are biodegradable and biocompatible. Amphiphiles of this kind can be obtained by designing molecules that are composed of biodegradable components. The cleavable (destructible) amphiphiles that contain a labile functional group have the potential to eliminate some of the above mentioned problems. Consequently, the self-assembly of PEGylated phospholipids[7,9] and synthetic nonionic amphiphiles with mPEG as head group[12–15] have attracted tremendous attention. This is because PEG has low cytotoxicity, flexible structure, and good water solubility. Further, the stealth effect of the so called hydrophilic PEG chain makes them useful in developing functional materials and drug delivery systems (DDS). Thus amphiphiles containing PEG chain have become a topic of interest due to their biocompatibility,[16–18] and ability to control particle aggregation in solution.[19]

Recently, our group has demonstrated room temperature self-assembly of low-molecular-mass ionic amphiphiles with mPEG tail and sulfonate ($-SO_3^-$), carboxylate ($-COO^-$), or ammonium ($-NR_3^+$) head group.[20–27] In fact, self-assembly of bolaamphiphiles with PEG as a spacer chain and zwitterionic or anionic head groups has also been reported. The PEG tail of these amphiphiles was found to act like a HC tail. These unconventional amphiphilic molecules self-assembled in water at room temperature in the same way as conventional amphiphiles do. We successfully demonstrated formation of different microstructures including spherical and disc-like micelles, and vesicles by these single PEG-tailed ionic amphiphiles. The work has been reviewed in a recent publication.[28] The extraordinary solution and self-organization properties of these amphiphiles led to the present investigation to study self-assembly of double mPEG-tailed amphiphiles in which both mPEG chains are of equal lengths. Thus sodium di-(mercaptopropanoyl poly(-ethylene glycol))-propane sulfonate with both mPEG chains of molar mass, M_n ~300 ($(mPEG_4)_2SO_3Na$) or M_n ~1100 ($(mPEG_{23})_2SO_3Na$) (see Fig. 1 for structures) were developed and characterized. In these molecules, the labile ester linkages connect the hydrophilic $-SO_3Na$ head and the so-called hydrophilic mPEG chains. Cleavage at the ester linkages converts the molecule into two non-amphiphilic products: an ionic and a neutral water-soluble compound. According to common notion the synthesized molecules ($(mPEG_4)_2SO_3Na$) and ($(mPEG_{23})_2SO_3Na$) containing two so-called hydrophilic mPEG chains are expected to be surface inactive and unable to produce self-assembled structures. Therefore, we were curious to see whether such molecules could self-organize like double hydrocarbon chain ionic surfactants in aqueous solution at room temperature. Thus solution behavior of the two newly developed amphiphiles was thoroughly investigated in aqueous buffer (pH 7.0) at 25 °C. The surface activity of the compounds in aqueous buffer was measured and compared with those of their corresponding single-chain analogues and commercial surfactants. The self-assembly behavior in aqueous solution was studied by use of various techniques including the steady-state fluorescence and NMR spectroscopy, dynamic light scattering (DLS), transmission electron microscopy (TEM), and atomic force microscopy (AFM). The thermodynamics of self-organization process was investigated by isothermal titration calorimetry (ITC) to determine the nature of driving force for self-association. The stability of the aggregates with respect to the change of temperature, concentration of additives, and ageing was also investigated.

2. Experimental section

2.1 Materials

Poly(ethylene glycol)methyl ether methacrylate (M_n ~300 ($mPEG_4$) and M_n ~1100 ($mPEG_{23}$)) and sodium 2,3-dimercaptopropanesulfonate monohydrate (95%) were purchased from Sigma-Aldrich (Bangalore, India). Triethylamine (TEA, 98%), sodium dihydrogen phosphate (≥99%), disodium monohydrogen phosphate (≥99%), sodium chloride (≥99%), and L-lysine hydrochloride salt were purchased from SRL (Mumbai, India). Methanol (MeOH) was obtained from Merck (Mumbai, India) and it was of analytical grade and was dried and distilled following typical procedures before use. All deuterated solvents, such as D_2O and CD_3OD were purchased from Cambridge Isotope Laboratories, Inc (CIL, India). Millipore filter paper was obtained from Merck, India. Milli-Q water (pH 6.7, resistivity 18 MΩ cm) was obtained from a Millipore water purifier (Elix, Bangalore, India).

The fluorescent probes such as *N*-phenyl-1-naphthylamine (NPN, 98%), 1,6-diphenyl-1,3,5-hexatriene (DPH, 98%), and pyrene (Py, 99%) were obtained from Sigma-Aldrich (Bangalore, India) and were purified by recrystallization from ethanol–water mixtures (80 : 20 v/v). The purity of the probes was checked by matching fluorescence excitation and absorption spectra.

The amphiphiles $(mPEG_4)_2SO_3Na$ and $(mPEG_{23})_2SO_3Na$ were synthesized by Michael addition reaction of sodium 2,3-dimercaptopropanesulfonate with poly(ethylene glycol)methyl ether methacrylate according to Scheme S1† following method reported in the literature.[20–27] The chemical structures of $(mPEG_4)_2SO_3Na$ and $(mPEG_{23})_2SO_3Na$ were determined by ^1H- and ^{13}C-NMR spectra (Fig. S1 and S2†). The synthesis procedure and chemical characterization have been included in ESI.†

2.2. Methods

Solution preparation. Aqueous stock solutions of $(mPEG_4)_2SO_3Na$ and $(mPEG_{23})_2SO_3Na$ were prepared in 20 mM phosphate buffer (pH 7.0, $I = 0.1$). For sample preparation, an aliquot of the stock solution was diluted using the same buffer at least 30 min before measurement. A saturated solution of NPN in pH 7.0 buffer was used for fluorescence titrations using NPN probe. For measurements using Py and DPH probes, stock solution (0.1 mM) was made in MeOH. An aliquot of this was diluted in phosphate buffer to achieve a final concentration of 1.0 μM. All measurements were carried out at 25 °C unless otherwise mentioned.

Instrumentation. The ^1H NMR measurements were performed using Bruker (AVANCE-III) and JEOL (ECA-500) operating at 400 MHz and 500 MHz FT-NMR spectrometers, respectively. Spin–lattice and spin–spin relaxation, and pulse field gradient (PFG) experiments were carried out on the 500 MHz FT-NMR spectrometer. A Shimadzu 1601 (Japan) double-beam UV-vis spectrophotometer was employed for the measurements of UV-vis absorbance spectra and transmittance (T), using a 1 cm^2 quartz cuvette. For pH measurements, an Instind Model ME (Kolkata, India) pH meter fitted with a glass electrode was employed. The pH meter was calibrated using standard buffers of known pH (7.0 and 4.0). For temperature controlled measurements, a Thermo Neslab RTE-7 (USA) circulating bath was employed.

Surface tension (ST) measurements were performed with a surface tensiometer (Model 3S, GBX, France) at 25 °C using Du Nuöy ring detachment method. A microcalorimeter from Microcal iTC_{200}, (made in U.S.A) was used for thermometric measurements.

A PerkinElmer LS-55 luminescence spectrometer equipped with a temperature-controlled cell holder and a polarization accessory that uses the L-format instrumental configuration was used to measure the steady-state fluorescence spectra of NPN and DPH probes. The fluorescence emission spectra of Py was recorded on a SPEX Fluorolog-3 (FL3-11, USA) spectrophotometer. An Optical Building Blocks Corporation Easylife instrument equipped with a nanosecond diode laser ($\lambda = 380$ nm) was used for the time-resolved fluorescence measurements.

A dynamic light scattering (DLS) spectrometer Zetasizer Nano ZS (Malvern Instrument Lab, Malvern, U.K.) fitted with a He–Ne laser operated at 4 mW at $\lambda_o = 632.8$ nm was employed to measure hydrodynamic size and size distribution of aggregates in solution. The same equipment was used also for surface zeta (ζ)-potential measurements.

High-resolution transmission electron micrographs were taken on an HRTEM (JEOL-JEM 2100, Japan) operating at an accelerating voltage of 200 kV, at room temperature. All AFM measurements were carried out by use of a Nanoscope IIIA from Digital Instruments (USA) in tapping mode under ambient conditions.

The details of all methods employed in this work can be found under ESI.†

3. Results and discussion

3.1 Surface activity

To examine whether $(mPEG_4)_2SO_3Na$ and $(mPEG_{23})_2SO_3Na$ can act like amphiphilic molecules we investigated their surface activity in phosphate buffer (20 mM, pH 7). The surface activity was measured by measuring surface tension (γ/mN m^{-1}) values of phosphate buffer in the presence of varying concentrations (C_s) of $(mPEG_4)_2SO_3Na$ or $(mPEG_{23})_2SO_3Na$. The results are presented in Fig. 2. It is observed that γ value decreases with the increase in C_s, showing amphiphilic nature of both $(mPEG_4)_2SO_3Na$ and $(mPEG_{23})_2SO_3Na$ at room temperature. The values of pC_{20} ($-\log C_{20}$, where C_{20} is the concentration of the amphiphiles required to reduce γ of buffer by 20 units) is *ca.* 2, which suggests that the molecules are weakly surface active in comparison to corresponding single HC tail surfactant.[29] In fact, the surface activity of both $(mPEG_4)_2SO_3Na$ and $(mPEG_{23})_2SO_3Na$ is even less than that of corresponding single mPEG-chain amphiphiles.[20–24] This means that the second mPEG chain enhances polarity of the molecule thereby reducing its amphiphilic character. This is reflected in the feature of the ST plots which is different from those of HC chain surfactants. Unlike conventional surfactants ST decreases over a wide concentration range without any clear inflection or breakpoint. However, the concentration ($\sim 3 \times 10^{-4}$ M) corresponding to the point as indicated by upward and downward arrows may be taken as the *cac* value.

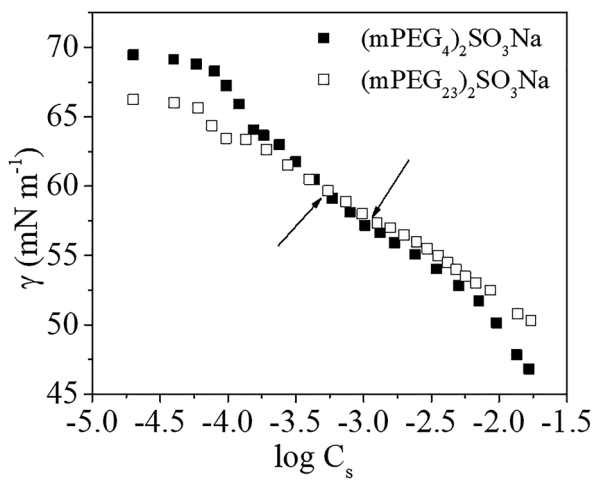

Fig. 2 Plots of variation of surface tension (γ) phosphate buffer (20 mM, pH 7) as a function of log C_s at 25 °C: (■) $(mPEG_4)_2SO_3Na$, (□) $(mPEG_{23})_2SO_3Na$.

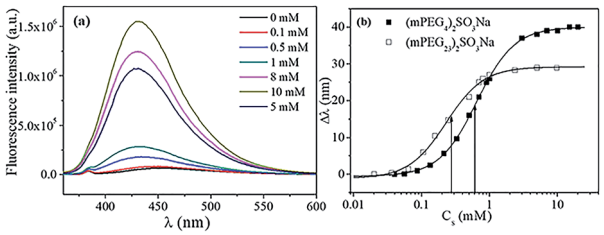

Fig. 3 (a) Representative fluorescence spectra of NPN in pH 7 buffer containing different concentrations of $(mPEG_4)_2SO_3Na$; (b) plots of spectral shift ($\Delta\lambda = \lambda_{max,water} - \lambda_{max,sample}$) of NPN as a function of C_s for $(mPEG_4)_2SO_3Na$ (■) and $(mPEG_{23})_2SO_3Na$ (□) in pH 7 buffer at 25 °C.

3.2 Self-assembly behavior

Fluorescence probe studies. The steady-state fluorescence spectrum of the hydrophobic molecule, NPN is known to be very sensitive to solvent polarity and viscosity change.[30] In polar solvents such as water, the fluorescence emission intensity of NPN is very weak and the emission maximum is highly red-shifted. But in a nonpolar solvent, the emission maximum exhibits a blue shift with a simultaneous rise in intensity. A similar phenomenon is also observed in aqueous solutions of conventional surfactants when surfactant concentration is increased above their respective *cac* value. Consequently, NPN has been widely exploited to study self-assembly of surfactants.[31–35] Therefore, the fluorescence spectra of NPN were measured in aqueous solutions in the presence of different concentrations (C_s) of both $(mPEG_4)_2SO_3Na$ and $(mPEG_{23})_2SO_3Na$. Representative spectra of NPN in solutions of $(mPEG_4)_2SO_3Na$ have been depicted in Fig. 3a. Notably, the emission maximum is observed to shift toward shorter wavelength with a concomitant rise of emission intensity with increasing concentration of $(mPEG_4)_2SO_3Na$. This suggests that both amphiphiles form aggregates of micropolarity much less than that of bulk water.[36] In other words, both $(mPEG_4)_2SO_3Na$ and $(mPEG_{23})_2SO_3Na$ behave like conventional HC tail surfactants at room temperature.

The plots of spectral shift ($\Delta\lambda = \lambda_{max,water} - \lambda_{max,sample}$) of NPN as a function of C_s are depicted in Fig. 3b. It is observed that the $\Delta\lambda$ value increases with C_s until a limiting value is reached corresponding to the plateau region. The sigmoidal feature of the curves clearly suggests a two-state process involving solubilization of NPN molecules within the less polar microdomains of aggregates. The concentration corresponding to the inflection point (indicated by arrows) can be taken as *cac* of the amphiphile. The *cac* values thus obtained are listed in Table 1. The slightly lower *cac* value of $(mPEG_{23})_2SO_3Na$ can be attributed to the conformational change of the longer mPEG tail. In fact, molecular dynamics (MD) simulations and spectroscopic data suggested random coil structure of longer PEG chain and helical structure of shorter PEG chain.[37] This means longer PEG chains are more flexible and the shorter PEG chains have stiff rod-like structure in an aqueous environment.

To estimate micropolarity of the aggregates formed by the amphiphilic molecules, we employed pyrene (Py) as a fluorescent probe. The ratio (I_1/I_3) of the intensities of the first (I_1) and third (I_3) vibronic peaks of the Py fluorescence spectrum has been shown to be sensitive to solvent polarity change and therefore has been used as a solvent polarity parameter.[38] The I_1/I_3 ratio is found to be large in water (1.79) and is small for hydrocarbon solvents (0.90).[38] Consequently, steady-state fluorescence spectra (Fig. S3†) of Py probe were recorded in aqueous solutions of $(mPEG_4)_2SO_3Na$ and $(mPEG_{23})_2SO_3Na$. The values of I_1/I_3 ratio are listed in Table 1. It is observed that the I_1/I_3 ratios of both amphiphiles are relatively higher than those of HC tail surfactants.[31–35] It should be noted that the I_1/I_3 ratio is also greater than the corresponding single mPEG-tailed amphiphiles.[20–24] Indeed, the microenvironments of Py molecules are polar like alcohol solvent,[38] indicating that Py molecules are partly exposed to aqueous environment. This is possible only if Py molecules are unable to penetrate into the core of aggregates and therefore are solubilized near the aggregate surface. This is substantiated by the results of NPN probe study which showed micropolarity of the aggregates is similar to those of micelles of HC chain surfactants.

To study the internal fluidity (microfluidity) of the aggregates, the steady-state fluorescence spectra of DPH, a water-insoluble hydrophobic probe, were measured in the presence of both $(mPEG_4)_2SO_3Na$ and $(mPEG_{23})_2SO_3Na$. The rise of emission intensity (not shown) indicates solubilization of the probe molecules within the much less polar microdomains of the aggregates formed by the amphiphiles. We also measured steady-state fluorescence anisotropy (r) of DPH probe in aqueous solutions containing different concentrations (>*cac*) of $(mPEG_4)_2SO_3Na$ and $(mPEG_{23})_2SO_3Na$. The relevant data can be found in Table S1.† The r value which is widely used as an index of microfluidity, is known to change when encapsulated within the hydrophobic microdomains of surfactant aggregates.[39] In the cases of $(mPEG_4)_2SO_3Na$ and $(mPEG_{23})_2SO_3Na$, the r value is observed to increase with concentration. It is important to note that the r values for both amphiphiles are much higher than that of SDS micelles ($r = 0.045$), but are comparable to many

Table 1 The self-association properties of $(mPEG_4)_2SO_3Na$ and $(mPEG_{23})_2SO_3Na$ in phosphate buffer (20 mM, pH 7) and fluorescence properties of DPH probe in solutions of $(mPEG_4)_2SO_3Na$ and $(mPEG_{23})_2SO_3Na$ at 25 °C

Surfactant	*cac* (mM)	I_1/I_3	η_m[a] (mPa s)	R_h[b] (nm)	ζ-Potential[b] (mV)
$(mPEG_4)_2SO_3Na$	0.6 ± 0.05	1.65 ± 0.03[a]	56.0 ± 1.0	200 ± 10	−16.00
$(mPEG_{23})_2SO_3Na$	0.3 ± 0.05	1.70 ± 0.04[a]	37.0 ± 1.0	75 ± 5	−7.61

[a] Measured using 5 mM solutions. [b] Measured using 2 mM solutions.

vesicle- or liposome-forming amphiphiles.[40,41] This suggests that both $(mPEG_4)_2SO_3Na$ and $(mPEG_{23})_2SO_3Na$ produce bilayer aggregates (*e.g.*, flat lamellar or vesicles) in buffer and the DPH molecules are solubilized within the tightly packed bilayer constituted by the mPEG chains (Fig. S4†). That the bilayer membrane is composed of mPEG chains is also suggested by the results of ζ-potential measurements as discussed below. In order to estimate rigidity of the bilayer, we have also estimated microviscosity (η_m) around DPH probe from its fluorescence lifetime (τ_f) and r values (Table S1†).[42] The higher η_m values compared to micellar aggregates of SDS (16.5 mPa s)[39] suggests formation of bilayer structures.

If the bilayer membrane is constituted by the mPEG chains, then the surface charge of the aggregates should be negative. The surface charge of the aggregates is usually measured by the ζ-potential value. The ζ-potential values of the bilayer aggregates in 2 mM solutions (pH 7) of $(mPEG_4)_2SO_3Na$ and $(mPEG_{23})_2SO_3Na$ were measured at different concentrations at 25 °C. The data are collected in Table 1. A significant negative ζ-potential value confirms that the outer surface of the aggregates is negatively charged and is constituted by the $-SO_3^-$ groups. This undoubtedly proves that the bilayer membrane of the aggregates is constituted by the mPEG chains.

3.3 Nuclear magnetic resonance studies

It is well-established that charged surfactant layers of arbitrary curvature such as a micelle, or a vesicle is stabilized by a balance of the hydrophobic effect which tends to decrease the interfacial area per surfactant (a) and electrostatic repulsions among head groups which tends to increase a.[43,44] However, later it was realized that an additional contribution arising from the effect of conformational entropy associated with the more or less flexible tails of a surfactant consisting of one or more aliphatic chains should also be considered.[45,46] Theoretical calculations have strongly suggested that when chain conformational entropy effects are taken into account single ionic surfactants with rigid tails preferentially form small micelles with a large curvature while ionic surfactants with a flexible tail form comparatively large aggregates with low curvature.[47] In fact, a pronounced flexibility of the tails of amphiphilic molecules appears to be a prerequisite for the formation of stable bilayer structures such as vesicles. It has been reported that the bending of a bilayer into a geometrically closed vesicle can only be formed by surfactants with flexible aliphatic chains.[47]

In the case of conventional surfactants, the self-assembly process is driven by the increase in entropy of the system due to breakdown of the highly ordered water structure around the HC chain (hydrophobic effect). The PEG/water system has also been shown to consist of mPEG chain surrounded by a sheath of water molecules, forming a loose coil of water molecules around the mPEG chain.[48,49] The water spiral is formed in such a way that more water molecules accumulate in the cavities surrounding the oxygen atoms of the mPEG chain.[50] The MD simulation and spectroscopic data suggest that the most likely conformation of mPEG chain is helical with –O– atoms stuck inside the helix and thus mPEG–water interactions are strong inside the helix.[37] To further verify this we have determined the mPEG chain conformation in water at room temperature by NMR spin-relaxation (T_1 and T_2) and self-diffusion measurements. The T_1 and T_2 values are sensitive to local and global dynamics, respectively, and provide rich dynamical information on the surfactants forming micelles.[51,52] The dynamics *via* T_1 is beneficial in extracting activation energy of molecular processes when T_1 is measured as a function of temperature. Therefore, T_1 and T_2 measurements were made using solutions of both $(mPEG_4)_2SO_3Na$ and $(mPEG_{23})_2SO_3Na$ and the data are listed in Tables S2 and S3 under ESI.† From the data in Table S2 (or Table S3†) it may be noted that, at any given temperature, $T_{1a} > T_{1b} > T_{1g}$ (for H_a, H_b and H_g protons; see Fig. S1†) which indicates their respective mobility in a decreasing fashion. For instance, higher T_{1a} reflects more mobile nature of H_a protons in $-OCH_3$ group, while H_g protons are experiencing somewhat restricted mobility. From spin-relaxation data measured at 500 MHz, an increasing tendency of both T_1 and T_2 against temperature can also be observed for $(mPEG_4)_2SO_3Na$ (Table S2†) and $(mPEG_{23})_2SO_3Na$ (Table S3†). An inspection of the data reveals

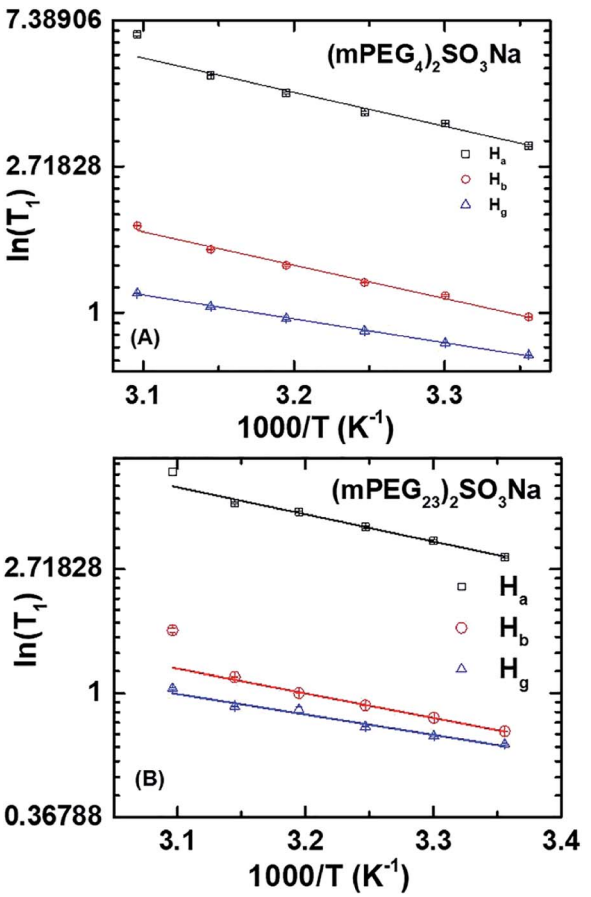

Fig. 4 Variable-temperature T_1 data for (A) $(mPEG_4)_2SO_3Na$ and (B) $(mPEG_{23})_2SO_3Na$; the solid line represents the best Arrhenius fit of the experimental data described by the eqn (1).

Table 2 Critical aggregation concentration (*cac*), change of standard molar Gibbs free energy (Δ_mG^o), enthalpy (Δ_mH^o) and entropy (Δ_mS^o) for the self-assembly process of $(mPEG_4)_2SO_3Na$ and $(mPEG_{23})_2SO_3Na$ in phosphate buffer (20 mM, pH 7.0) at 25 °C

Surfactant	*cac* (mM)	Δ_mG^o (kJ mol^{-1})	Δ_mH^o (kJ mol^{-1})	Δ_mS^o (JK^{-1}mol^{-1})	$T\Delta_mS^o$ (kJ mol^{-1})
$(mPEG_4)_2SO_3Na$	1.7 ± 0.1	−28.45	0.25	96	28.70
$(mPEG_{23})_2SO_3Na$	0.4 ± 0.1	−34.90	0.68	119	35.58

that T_1 and T_2 values are not significantly different from each other, which facilitates the analysis of relaxation data in the frame of fast motions.[52,53] Hence the obtained T_1's are well described by an Arrhenius fit described by the equation:[53]

$$T_1 = Ae^{-E_a/RT} \quad (1)$$

where A is a constant, E_a is the activation energy and other symbols have their usual meaning. A plot of $\ln(T_1)$ *vs.* $1000/T$ yielding the activation energies (E_as) of 19.5 kJ mol^{-1}, 19.1 kJ mol^{-1} and 13.6 kJ mol^{-1} for H_a, H_b and H_g, respectively, for $(mPEG_4)_2SO_3Na$ (Fig. 4A). In a similar fashion, for $(mPEG_{23})_2SO_3Na$ (Fig. 4B), the E_as obtained are 18.2 kJ mol^{-1}, 16.6 kJ mol^{-1} and 13.8 kJ mol^{-1} for H_a, H_b and H_g, respectively. In general, an activation energy of ~15 kJ mol^{-1} is a good indication of *trans–gauche* conformation changes within hydrocarbon chains of surfactants.[54] Hence, the obtained E_as for both $(mPEG_4)_2SO_3Na$ and $(mPEG_{23})_2SO_3Na$ reflect *gauche–trans* conformational changes and is consistent with previous reports.[54,55] It is interesting to note that the E_as noted are well corroborated with the results of MD simulations.[37]

That the PEG chains assumes helical conformation in water is confirmed by the results of diffusion NMR experiments. Details are described under ESI.† The extracted self-diffusion coefficients for $(mPEG_4)_2SO_3Na$ and $(mPEG_{23})_2SO_3Na$ (Fig. S5†) are 3.53 × 10^{-10} m^2 s^{-1} and 1.74 × 10^{-10} m^2 s^{-1}, corresponds to hydrodynamic radius, R_h equal to 0.56 and 1.14 nm, respectively. Nevertheless, a deviation from single-exponential decay is observed for $(mPEG_{23})_2SO_3Na$ portrayed in Fig. S5.† In this regard, a biexponential fit with two diffusion coefficients is a reasonable description of diffusion data of $(mPEG_{23})_2SO_3Na$. The two diffusitivies with D equal to 2.22 × 10^{-10} m^2 s^{-1} and 0.91 × 10^{-10} m^2 s^{-1} corresponding to R_h values 0.90 and 2.19 nm, respectively, can be associated with the rigid helical and flexible random coil structures of $(mPEG_{23})_2SO_3Na$ at equilibrium. It is interesting to note that the amphiphiles do not form aggregates in D_2O at the concentration (1 mM) employed for the experiments which is confirmed by the diffusion constants and the respective R_h values.

3.4 Thermodynamics of vesicle formation

In order to understand the self-assembly process of $(mPEG_4)_2SO_3Na$ and $(mPEG_{23})_2SO_3Na$, we measured thermodynamic parameters such as standard free energy (Δ_mG^o), enthalpy (Δ_mH^o), and entropy (Δ_mS^o) of micellization at 25 °C using ITC. The titration curves are depicted in Fig. S6† under ESI. The *cac* and Δ_mH^o values were directly obtained from the inflection point of respective plot. The other thermodynamic parameters, Δ_mG^o and Δ_mS^o associated with the micellization process were calculated using pseudophase separation model.[56] The thermodynamic data are collected in Table 2. The Δ_mG^o values are found to be negative, which imply spontaneous aggregation of the amphiphiles. The $T\Delta_mS^o$ value calculated from the respective Δ_mS^o value is observed to be much higher than the corresponding Δ_mH^o value. This means that the aggregate formation by both amphiphiles is driven by positive entropy change associated with the hydrophobic effect as well as conformational change of the mPEG chains. The contribution of conformational entropy to Δ_mG^o is reflected by the higher Δ_mS^o value in case of $(mPEG_{23})_2SO_3Na$ that has relatively longer mPEG chains.

3.5 Size and shape of vesicles

The hydrodynamic size distribution of the aggregates formed in 2 mM $(mPEG_4)_2SO_3Na$ and $(mPEG_{23})_2SO_3Na$ are presented in Fig. 5 and the mean R_h values thus obtained are collected in Table 1. Though a bimodal distribution is observed in the case of $(mPEG_4)_2SO_3Na$, the volume percentage of smaller aggregates is much less than the larger aggregates. It is interesting to note that mean R_h value of the aggregates of $(mPEG_4)_2SO_3Na$ is less than that of $(mPEG_{23})_2SO_3Na$. The morphology of the aggregates can be visualized in the HRTEM images of the buffered

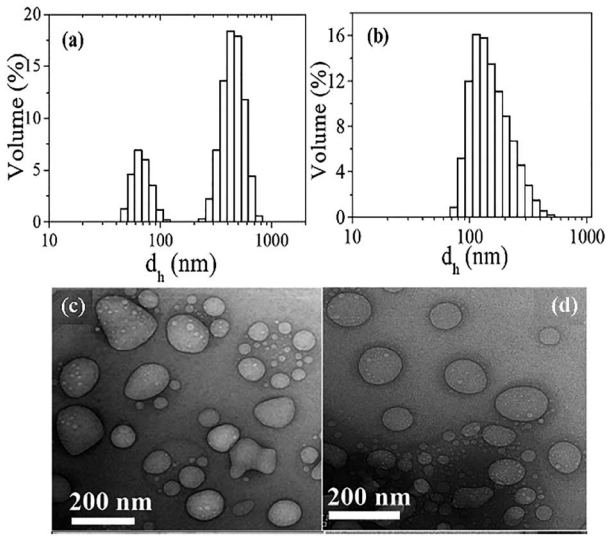

Fig. 5 Upper panel: Size distribution histograms of aggregates in 2.0 mM solutions (pH 7) of (a) $(mPEG_4)_2SO_3Na$, and (b) $(mPEG_{23})_2SO_3Na$ at 25 °C; lower panel: unstained HRTEM images of 2 mM (c) $(mPEG_4)_2SO_3Na$ and (d) $(mPEG_{23})_2SO_3Na$ solutions in phosphate buffer (pH 7.0).

solutions of the amphiphiles. The corresponding HRTEM images of the unstained specimens have been shown in Fig. 5. The micrographs clearly reveal existence of vesicles of R_h in the range of 50–100 nm in 2 mM solution of both amphiphiles. It should be noted that the size of the vesicles is slightly smaller than that obtained by DLS measurements. However, this is very common with the conventional HRTEM measurements that involve drying of the samples. The results of DLS and HRTEM measurements are thus consistent with the results of fluorescence probe studies that predicted existence of bilayer aggregates. Though the bilayer thickness of the vesicles could not be measured, the presence of aqueous core surrounded by a thin membrane suggests existence of small unilamellar vesicles (SUVs) in solutions of the amphiphiles.

The existence of spherical aggregates can also be observed in the AFM images as shown in Fig. 6. In both images, well-defined spherical structures with R_h values in the range 25–125 nm for $(mPEG_4)_2SO_3Na$ and 40–75 nm for $(mPEG_{23})_2SO_3Na$ can be detected which agree well with the results obtained by HRTEM. The height profile obtained using AFM is representative of the thickness of two closely stacked membranes tilted together after drying and collapse of the vesicles. Consequently, half of the thickness can be considered as the thickness of the vesicle membrane. That is, the height of ~8 nm corresponds to a membrane thickness of 4 nm (Fig. 6). From the ChemDraw energy-minimized structure analysis the length of the mPEG tails of $(mPEG_4)_2SO_3Na$ molecule is found to be ~1.9 nm, which is about one half of the membrane thickness confirming bilayer vesicle formation by the $(mPEG_4)_2SO_3Na$ molecules. The same is also true with $(mPEG_{23})_2SO_3Na$ amphiphile for which the height obtained is equal to ~17 nm and the calculated fully-extended length of the mPEG chains is ~8.5 nm. That is, the bilayer membrane thickness of the vesicles of $(mPEG_{23})_2SO_3Na$ amphiphile is exactly twice the mPEG chain length. This also suggests that the helical structure of the mPEG chains in free $(mPEG_4)_2SO_3Na$ or $(mPEG_{23})_2SO_3Na$ molecules gets stretched leading to the formation of random coil structure upon aggregation.

3.6 Stability of vesicles

Effect of temperature. For practical applications, the vesicles should have sufficient physical stability under physiological conditions (pH 7.4, 37 °C). Therefore, the effect of temperature on their stability in phosphate buffer (pH 7) was studied using DPH probe the r value of which is sensitive to change in microviscosity. The r values of DPH in 5 mM $(mPEG_4)_2SO_3Na$ or $(mPEG_{23})_2SO_3Na$ solutions were measured in the temperature range 25–75 °C and the results are presented in Fig. S7a.† The plots of both the amphiphiles show a gradual fall of r value with increasing temperature, indicating decrease in microviscosity with the rise in temperature as a result of weakening of the hydrophobic interaction and other weak physical forces that are responsible for forming vesicles. This results in a phase transition of the bilayer membrane from more rigid gel state to a more fluid liquid-crystalline state. Thus the temperature corresponding to the inflection point of the sigmoidal curves can be taken as the phase transition temperature, T_m. The T_m values of $(mPEG_4)_2SO_3Na$ (51 °C) and $(mPEG_{23})_2SO_3Na$ (51 °C) are consistent with the stronger interactions among mPEG chains in the vesicle bilayer at room temperature. It is important to note that unlike PEGylated polymers,[57] clouding phenomenon (LCST) was not observed even at 75 °C. In other words, the vesicles produced by $(mPEG_4)_2SO_3Na$ and $(mPEG_{23})_2SO_3Na$ amphiphiles are highly stable at the physiological temperature (37 °C), thereby making them good candidates for use as DDSs in pharmaceutical industry.

Effect of aging. In order to investigate the shelf-life of the vesicles, the turbidity ($\tau = 100 - \%T$) of 1 mM solutions (pH 7.0) of $(mPEG_4)_2SO_3Na$ and $(mPEG_{23})_2SO_3Na$ was measured at 37 °C at different time intervals during 60 days. The experimental results are presented in Fig. S7b.† The plots reveal that the turbidity initially increases only slightly with time, reaching almost a steady value after 60 days. The initial increase in turbidity could be due to the formation and/or growth of the vesicles, while the subsequent plateau refers to the storage life of the vesicles. Thus, the vesicles produced by the double mPEG-tailed amphiphiles exhibit excellent stability at the physiological temperature at least for two months.

Salt-induced morphological transition. As the surfactants are anionic in nature there might be a significant effect of salt concentration on the aggregation behavior of the surfactants. It is well known that the addition of counter ion usually induces

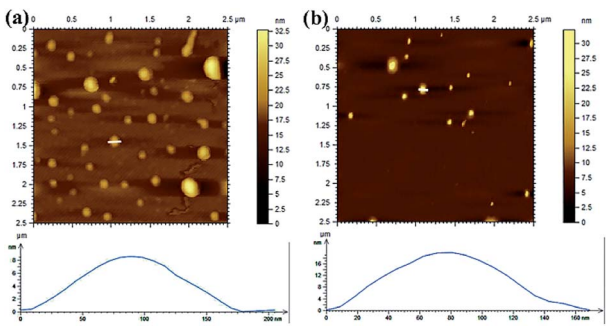

Fig. 6 AFM images (upper panel) with scale-bar and height distribution (lower panel) of the aggregates in 2 mM solutions of (a) $(mPEG_4)_2SO_3Na$ and (b) $(mPEG_{23})_2SO_3Na$ in pH 7.0.

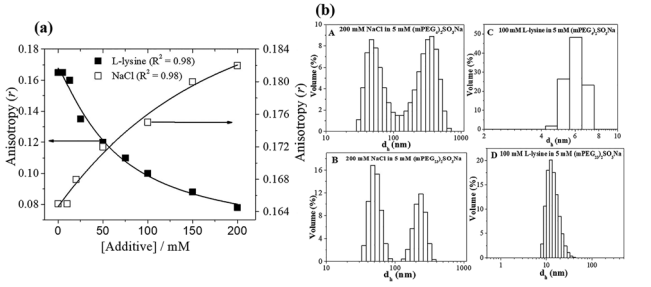

Fig. 7 (a) Variation of r in 5 mM $(mPEG_4)_2SO_3Na$ with concentration of NaCl (□) and L-lysine hydrochloride (■); (b) size distribution histograms of solutions of 5 mM $(mPEG_4)_2SO_3Na$ containing 200 mM NaCl (A), 5 mM $(mPEG_{23})_2SO_3Na$ containing 200 mM NaCl (B), 5 mM $(mPEG_4)_2SO_3Na$ containing 100 mM L-lysine hydrochloride (C), and 5 mM $(mPEG_{23})_2SO_3Na$ containing 100 mM L-lysine hydrochloride (D).

transition of vesicle to other structures.[58–61] To investigate the influence of salt concentration on aggregate morphology, the *r* value of DPH probe was measured in solution of $(mPEG_4)_2SO_3Na$ in the presence of varying concentration of NaCl. The plot of variation of *r* with [NaCl] can be found in Fig. 7a. The plot shows a slight increase of *r* value with the rise of NaCl concentration, suggesting transformation of SUVs to more ordered structures. The size distribution histograms (Fig. 7b) of the vesicles in 5 mM $(mPEG_4)_2SO_3Na$ or $(mPEG_{23})_2SO_3Na$ solutions containing 200 mM NaCl show that the mean R_h value is higher than the value obtained in the absence of salt. Since no significant increase in solution viscosity is observed, this can be associated with the transformation of SUVs to large multilamellar vesicles (MLVs), tubules, or disk-like aggregates. Indeed the TEM micrograph of the 5 mM solution (containing 200 mM NaCl) of the amphiphiles shows formation tubular aggregates (Fig. 8a) in the case of $(mPEG_4)_2SO_3Na$ and large disk-like micelles in the case of $(mPEG_{23})_2SO_3Na$ (Fig. 8c). The tube-like aggregates have inner diameter of ~50–100 nm. This can be attributed to tight packing of the mPEG chains caused by the removal of ionic repulsion upon addition of salt.

Surprisingly, addition of L-lysine hydrochloride was observed to have significant effect on the stability of the SUVs formed by both the amphiphilic molecules. The plot of *r* of DPH in 5 mM $(mPEG_4)_2SO_3Na$ as a function of [L-lysine hydrochloride] is presented in Fig. 7a which shows an exponential fall of *r* value with the increase of [L-lysine hydrochloride], indicating transformation of bilayer structure to some less ordered structures. Also, the size distribution histograms (Fig. 7b) of aggregates in 5 mM $(mPEG_4)_2SO_3Na$ and $(mPEG_{23})_2SO_3Na$ solution containing 100 mM L-lysine hydrochloride show the presence of aggregates with mean R_h < 5 nm. The corresponding TEM images (Fig. 8b and d) which show existence of very small micelles-like aggregates for both the amphiphiles are consistent with the results of DLS and fluorescence probe measurements. The transformation of bilayer vesicles to small micelles with the increase of [L-lysine hydrochloride] can be attributed to the strong electrostatic attraction among the negatively charged $-SO_3^-$ head group of the surfactant molecules and large, positively charged L-lysinium cations. Strong electrostatic interaction of the L-lysinium cation with the $-SO_3^-$ head group results in a complete destruction of vesicles forming small micellar aggregates. This kind of behavior has also been observed with single-tailed amphiphiles having $-SO_3^-$ head. The results of this experiment suggest that L-lysinium cation can be used to induce release of drug molecules encapsulated by the vesicles in solutions of $(mPEG_4)_2SO_3Na$ and $(mPEG_{23})_2SO_3Na$ amphiphiles.

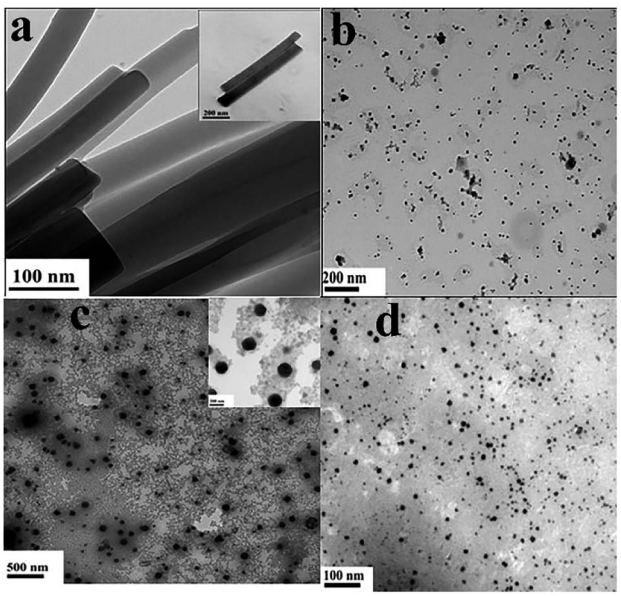

Fig. 8 HRTEM images of 5 mM $(mPEG_4)_2SO_3Na$ containing (a) 200 mM NaCl, (b) 100 mM L-lysine hydrochloride; and 5 mM $(mPEG_{23})_2SO_3Na$ containing (c) 200 mM NaCl, (d) 5 mM 100 mM L-lysine hydrochloride; inset (a): one section analysis; inset (c): one section analysis.

4. Conclusions

In summary, two novel unconventional double mPEG-tailed amphiphiles $(mPEG_4)_2SO_3Na$ and $(mPEG_{23})_2SO_3Na$ with $-SO_3^-$ head group were developed and characterized. The mPEG chains of $(mPEG_4)_2SO_3Na$ and $(mPEG_{23})_2SO_3Na$, respectively assumes a helical and random coil conformation in water such that more water molecules accumulate in the cavities surrounding the oxygen atoms of the mPEG chain. Despite having two so called polar mPEG tails and an anionic ($-SO_3^-$) head group both molecules were found to be surface active in water. Also, both $(mPEG_4)_2SO_3Na$ and $(mPEG_{23})_2SO_3Na$ were observed to have a strong tendency to self-assemble in aqueous buffered solution above a low *cac* at room temperature. The self-assembly process is accompanied by a conformational change of the mPEG chains of the amphiphilic molecules. To the best of our knowledge this is the first report on the self-assembly of double mPEG-chain containing anionic amphiphiles. The double mPEG-tailed amphiphiles exhibit formation of SUVs in dilute solutions. The polar mPEG chains of these amphiphiles behave like hydrocarbon tails of conventional double-tail surfactants and constitute the bilayer membrane of the vesicle. The driving force behind the vesicle formation is the well-known hydrophobic effect that is entropy gain by the system due to breakdown of the iceberg water structure inside the helical cavity of the mPEG chain which leads to stretching of the mPEG chain in the vesicle bilayer. Interestingly, unlike PEGylated polymers, the amphiphiles do not exhibit clouding phenomenon (LCST) even at 75 °C. Thus, vesicles produced by $(mPEG_4)_2SO_3Na$ and $(mPEG_{23})_2SO_3Na$ amphiphiles are highly stable at the physiological temperature. Also, the SUVs of $(mPEG_4)_2SO_3Na$ and $(mPEG_{23})_2SO_3Na$ are found to be stable for at least two months at the physiological temperature. However, in the presence of NaCl, the vesicles of both amphiphiles are transformed into either tubules or disk-like aggregates. But, in the presence of L-lysine hydrochloride salt the SUVs are transformed into small micelles. The vesicle-to-micelle transition can find application in L-lysinium cation-triggered delivery of drug molecules. Further, these amphiphilic molecules have hydrolysable ester bonds which can be cleaved in acidic pH

thereby releasing encapsulated drug molecules. As $(mPEG_4)_2$-SO_3Na and $(mPEG_{23})_2SO_3Na$ are biodegradable and mPEG is an FDA approved molecule, we believe that they can have potential uses in the biomedical sciences and pharmaceutical industries.

Conflicts of interest

The authors declare no competing financial interests.

Acknowledgements

The authors acknowledge financial support from the SERB-DST project (Grant no. SR/S1/PC-68/2008), and Indian Institute of Technology Kharagpur, India. We also thank Dr Subhajit Ghosh (IIT Guwahati, India) and Dr N. Sarkar for assistance with the calorimetric and DLS measurements, respectively.

Notes and references

1 M. J. Rosen. *Surfactants and Interfacial Phenomena*, Wiley-Interscience, New York, 4th edn, 2004.
2 E. Smulders, in *Laundry detergents*, ed. E. Smulders, Wiley-VCH, New York, 2002, part 3, pp. 38–98.
3 J. H. Fendler, *Membrane Mimetic Chemistry*, Wiley, New York, 1982, ch. 6.
4 R. G. Laughlin, *The Aqueous Phase BehaVior of Surfactants*, Academic Press, London, UK, 1997.
5 W. M. Gelbart, A. Ben-Shaul and D. Roux, *Micelles, Membranes, Microemulsions, and Monolayers*, Springer-Verlag, New York, 1994.
6 D. F. Evans and H. Wennerström, *The Colloidal Domain*, Wiley-VCH, New York, 2nd edn, 1999.
7 G. Cevc, and D. Marsh, *Phospholipid Bilayers. Physical Principles and Models*, Wiley-Interscience, New York, 1987.
8 D. Marsh, *Biophys. J.*, 2012, **102**, 1079–1087.
9 J. Li, X. Wang, T. Zhang, C. Wang, Z. Huang, X. Luo and Y. Deng, *Asian J. Pharm. Sci.*, 2015, **10**, 81–98.
10 N. Skar-Gislinge, N. T. Johansen, R. Høiberg-Nielsen and L. Arleth, *Langmuir*, 2018, **34**, 12569–12582.
11 K. Aramaki, J. Yamada, Y. Tsukijima, T. Maehara, D. Aburano, Y. Sakanishi and K. Kitao, *Langmuir*, 2015, **31**, 10664–10671.
12 G. S. Kwon and T. Okano, *Adv. Drug Delivery Rev.*, 1996, **21**, 107–116.
13 M. G. Carstens, C. F. van Nostrum, A. Ramzi, J. D. Meeldijk, R. Verrijk, L. L. de Leede, D. J. A. Crommelin and W. E. Hennink, *Langmuir*, 2005, **21**, 11446–11454.
14 V. S. Trubetskoy and V. P. Torchilin, *Adv. Drug Delivery Rev.*, 1995, **16**, 311–320.
15 A. L. Klibanov, K. Maruyama, V. P. Torchilin and L. Huang, *FEBS Lett.*, 1990, **268**, 235–238.
16 S. Rex, M. J. Zuckermann, M. Lafleur and J. R. Silvius, *Biophys. J.*, 1998, **75**, 2900–2914.
17 E. Evans and W. Rawicz, *Phys. Rev. Lett.*, 1997, **79**, 2379–2382.
18 R. Ghosh and J. Dey, *Langmuir*, 2020, **36**(21), 5829–5838.
19 W. C. K. Poon, A. D. Pirie, M. D. Haw and P. N. Pusey, *Phys. A*, 1997, **235**, 110–119.
20 J. Dey and S. Shrivastava, *Soft Matter*, 2012, **8**, 1305–1308.
21 R. Ghosh and J. Dey, *J. Colloid Interface Sci.*, 2015, **451**, 53–62.
22 J. Dey and S. Shrivastava, *Langmuir*, 2012, **28**, 17247–17255.
23 R. Ghosh and J. Dey, *Langmuir*, 2017, **33**, 543–552.
24 R. Ghosh and J. Dey, *Langmuir*, 2014, **30**, 13516–13524.
25 S. Ghosh, R. Das Mahapatra and J. Dey, *Langmuir*, 2014, **30**, 1677–1685.
26 R. Das Mahapatra and J. Dey, *Langmuir*, 2015, **31**, 8703–8709.
27 R. Ghosh and J. Dey, *Langmuir*, 2017, **33**, 7741–7750.
28 J. Dey, R. Ghosh and R. Das Mahapatra, *Langmuir*, 2019, **35**, 848–861.
29 C. Tanford, *Science*, 1978, **200**, 1012–1018.
30 T. Saitoh, K. Taguchi and M. Hiraide, *Anal. Chim. Acta*, 2002, **454**, 203–208.
31 A. Mohanty and J. Dey, *Langmuir*, 2004, **20**, 8452–8459.
32 S. Roy, D. Khatua and J. Dey, *J. Colloid Interface Sci.*, 2005, **292**, 255–264.
33 S. Roy and J. Dey, *Langmuir*, 2005, **21**, 10362–10369.
34 A. Mohanty and J. Dey, *Langmuir*, 2007, **23**, 1033–1040.
35 T. Patra, S. Ghosh and J. Dey, *J. Colloid Interface Sci.*, 2014, **436**, 138–145.
36 E. D. Cehelnik, J. R. Cundall, J. R. Lockwood and T. F. Palmer, *J. Phys. Chem.*, 1975, **79**, 1369.
37 H. Lee, A. H. de Vries, S.-J. Marrink and R. W. Pastor, *J. Phys. Chem. B*, 2009, **113**, 13186–13194.
38 K. Kalyanasundaram and J. K. Thomas, *J. Am. Chem. Soc.*, 1977, **99**, 2039–2044.
39 S. Roy, S. Mohanty and J. Dey, *Chem. Phys. Lett.*, 2005, **414**, 23–27.
40 G. Weber, M. Shinitzky, A. C. Dianoux and C. Gitler, *Biochemistry*, 1971, **10**, 2106–2113.
41 M. Shinitzky and I. Yuli, *Chem. Phys. Lipids*, 1982, **30**, 261–282.
42 J. R. Lakowicz, *Principles of Fluorescence Spectroscopy*, Plenum Press, New York, 1983, p. 132.
43 J. N. Israelachvili, D. J. Mitchell and B. W. Ninham, *J. Chem. Soc., Faraday Trans. 2*, 1976, **72**, 1525–1568.
44 C. Tanford, *The hydrophobic effect*, Wiley, New York, 1980.
45 D. W. R. Gruen, and E. H. B. Lacey, in *Surfactants in Solution*, K. L. Mittal and B. Lindman, Plenum, New York, 1984, vol. I, pp. 279–306.
46 A. Ben-Shaul, I. Szleifer and W. M. Gelbart, *J. Chem. Phys.*, 1985, **83**, 3597–3611.
47 L. M. Bergström, *Langmuir*, 2006, **22**, 3678.
48 M. Ataman, *J. Macromol. Sci., Part A: Pure Appl. Chem.*, 1987, **24**, 967–976.
49 S. Kawaguchi, G. Imai, J. Suzuki, A. Miyahara, T. Kitano and K. Ito, *Polymer*, 1997, **38**, 2885–2891.
50 M. L. Alessi, A. I. Norman, S. E. Knowlton, D. L. Ho and S. C. Greer, *Macromolecules*, 2005, **38**, 9333–9340.
51 B. V. N. Phani Kumar, U. S. Priyadharsini, G. K. S. Prameela and A. B. Mandal, *J. Colloid Interface Sci.*, 2011, **360**, 154–162.
52 O. Söderman, P. Stilbs and W. S. Price, *Concepts Magn. Reson., Part A*, 2004, **23**, 121–135.
53 R. K. Harris, *Nuclear Magnetic Resonance Spectroscopy*, Longman, London, 1986.

54 P. J. Bratt, D. G. Gillies, L. H. Sutcliffe and A. J. Williams, *J. Phys. Chem.*, 1990, **94**, 2727–2729.
55 G. K. S. Prameela, B. V. N. Phani Kumar, V. K. Aswal and A. B. Mandal, *Phys. Chem. Chem. Phys.*, 2013, **15**, 17577–17586.
56 P. Majhi and S. Moulik, *Langmuir*, 1998, **14**, 3986–3990.
57 P. Wei, T. R. Cook, X. Yan, F. Huang and P. J. Stang, *J. Am. Chem. Soc.*, 2014, **136**, 15497–15500.
58 D. Yu, X. Huang, M. Deng, Y. Lin, L. Jiang, J. Huang and Y. Wang, *J. Phys. Chem. B*, 2010, **114**, 14955–14964.
59 X. Wang, J. Zhu, J. Wang and G. Zeng, *J. Dispersion Sci. Technol.*, 2008, **29**, 83–88.
60 Y. Yan, W. Xiong, X. Li, T. Lu, J. Huang, Z. Li and H. Fu, *J. Phys. Chem. B*, 2007, **111**, 2225–2230.
61 S. J. Ryhänen, V. M. J. Säily, M. J. Parry, P. Luciani, G. Mancini, J. M. I. Alakoskela and P. K. J. Kinnunen, *J. Am. Chem. Soc.*, 2006, **128**, 8659–8663.